Urol Res (2010) 38:477–484
DOI 10.1007/s00240-010-0326-x

SYMPOSIUM PAPER

Micro-computed tomography for analysis of urinary calculi

James C. Williams Jr. · James A. McAteer · Andrew P. Evan · James E. Lingeman

Received: 28 September 2010 / Accepted: 1 October 2010 / Published online: 22 October 2010

Abstract Micro-computed tomographic (micro CT) imaging has become an important tool for the study of urinary stones. The method involves the collection of a series of X-ray pictures of the stone as it is rotated, and the internal structure of the stone is computationally reconstructed from these pictures. The entire process takes from 30 min to an hour with present technology. Resulting images of the stone provide unprecedented detail of the mineral composition and its morphological arrangement within the stone. For smaller stones, reconstructions can easily have voxel sizes of <5 μm, making this a truly microscopic view of the stone. The micro CT reconstructions can be viewed with any of a number of existing methods for visualizing the structure of both the surface and internal features of the stone. Because the entire process is non-destructive, traditional analysis methods—such as dissection and spectroscopic examination of portions of the stones—can also be performed. Micro CT adds value to traditional methods by identifying regions of the stone to be analyzed, and also with its ability to scan a cluster of stones or stone fragments at once. Finally, micro CT has become a powerful tool to help investigate events in stone formation that distinguish different kinds of stone disease.

Keywords Calculi · Stone composition · Urolithiasis

Proceedings paper from the 3rd International Urolithiasis Research Symposium, Indianapolis, Indiana, USA, December 3–4, 2009.

J. C. Williams Jr. (✉) · J. A. McAteer · A. P. Evan
Department of Anatomy and Cell Biology,
Indiana University School of Medicine,
635 Barnhill Drive MS 5055Y,
Indianapolis, IN 46202-5120, USA
e-mail: jwillia3@iupui.edu

J. E. Lingeman
Methodist Hospital Institute for Kidney Stone Disease,
Indianapolis, IN, USA

Introduction

Micro-computed tomographic imaging (micro CT) utilizes X-rays to produce three-dimensional images with microscopic resolution [1–3]. It was first applied to kidney stones by Cleveland et al. [4] who used micro CT to characterize the breakage of a stone by shock waves. Soon after that, it was reported that different mineral types could be distinguished using micro CT [5, 6]. Since that time, several studies have utilized micro CT for its ability to non-destructively analyze urinary stones [7–15].

In this paper, we review the use of micro CT in the study of urinary stones. Micro CT is able to reveal structure within stones to a resolution of just a few micrometers, and a number of mineral types can be accurately distinguished from one another with high spatial resolution. In addition, micro CT allows the screening of large numbers of fragments from a patient so that fragments of distinctive composition can be identified much more easily than by visual inspection. Identification of distinctive regions of a single stone specimen can be beneficial for dissection purposes. For either a group of fragments or for dissection of a single stone, micro CT thus can provide guidance for collecting specimens for further analysis by other means such as Fourier-transform infrared spectroscopy (FT-IR). Finally, we show that micro CT can provide structural/compositional information which can be used to understand the etiologies of stone formation.

Basics of micro CT imaging

The essence of micro CT is similar to CT used clinically, but with several significant differences. While in clinical CT the X-ray source and detector are spun around the patient, in micro CT the specimen is rotated within the stationary X-ray beam (Fig. 1). This rotation is done in discrete steps, making it more like the old 'step-and-shoot' CT systems than the newer helical CT technologies. The size of the specimen is limited to a few centimeters in micro CT, and to obtain the high-resolution characteristic of micro CT, the intensities of X-rays are high and the exposure times are long, making this kind of micro CT inappropriate for living things (although some intermediate-resolution forms of micro CT are designed for scanning laboratory animals [16]). For the images shown in this paper, scanning times ranged from 30 to 60 min in length, typically for the collection of 450 X-ray images, with the specimen rotated 0.4° between each image.

The 'tomographic' part of micro CT involves taking the series of X-ray images of the specimen and calculating what arrangement of X-ray-absorbing materials would yield such a series (Fig. 2). The most commonly used method for making this calculation is that developed by Feldkamp et al. [17]. Improvements in computing power mean that this calculation—or 'reconstruction'—can be done during the time the next specimen is being scanned. Our Skyscan 1172 system utilizes a bank of four computers to do this, and the reconstruction software feeds each computer the data for reconstruction of a single slice, so that the system reconstructs four slices at a time, greatly speeding up the reconstruction process.

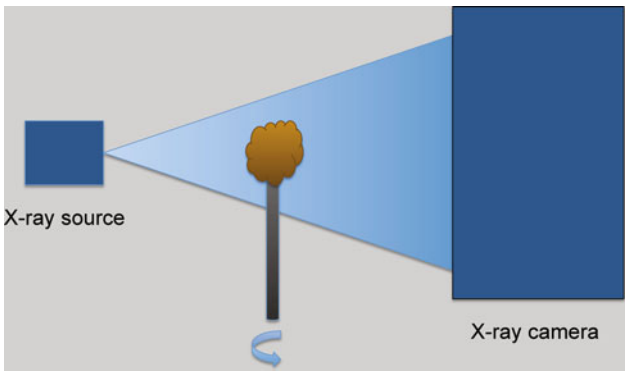

Fig. 1 Basics of a typical micro CT system include an X-ray source—in this case one that produces a cone-shaped beam—and a detector, which in newer systems consists of a solid-state X-ray camera. The specimen is positioned into the path of the X-ray beam and a picture of the 'shadow' image is captured. The specimen is then rotated a fraction of a degree and another image captured. This is repeated until the specimen has been rotated at least 180°. The set of X-ray images is then processed by computer to yield images of the internal structure of the specimen

High-resolution distinction of stone components

Figure 3 shows a reconstructed slice through the stone given as an example in Fig. 2. In this kind of calcium oxalate stone, the dihydrate form (COD) has distinctly lower X-ray attenuation (darker gray) than does the monohydrate (COM). The sharpness of the crystal edges and the evenness of the X-ray attenuation (gray level) of the COD crystals also suggests that they are pure and recently formed [18]. In looking at these crystals with a surface rendering (Fig. 4), they show the interpenetration twinning that has been previously described using scanning electron microscopy (SEM) [18, 19].

The arrowhead in Fig. 3 indicates a region within the COD that has undergone conversion to COM. We make this identification by comparison with work by others who have identified these structures using other methods [20–22]. We have seen these regions commonly within COD crystals. Their appearance by micro CT—showing X-ray attenuation similar to that seen for COM elsewhere in the same stone, and regions of low attenuation between the 'island' of COM and the surrounding COD—is strikingly similar to images published by Domingo-Neumann et al. [22] using SEM and backscatter imaging.

The region of apatite in this stone (Fig. 3) in three dimensions is a flat, elongated disk 100–200 μm thick (data not shown). Part of this apatite extends out to an indented region of the stone's surface, suggesting that the stone began on Randall's plaque [9].

In all, the details of this stone visible by micro CT are many, and the resolution is microscopic. Because micro CT produces a stack of image slices with the spatial distance between image slices being the same as the width and height of each pixel in the images (i.e., cubic image voxels), the stack can be resliced in any plane to obtain equivalently fine resolution for the examination of any structure, regardless of its orientation during the original scan.

Identifying regions of interest for analysis by other methods

Often the micro CT scan of a stone can provide information about which region or regions of the stone or stone fragments should be investigated for analysis by other methods (such as FT-IR). Indeed, we are finding that micro CT can reveal more regions within a single stone that we presently are capable of properly dissecting and identifying by other methods. The stone illustrated in Fig. 5 shows more than half-dozen distinctive regions by micro CT, and not all of them could be successfully isolated for further analysis.

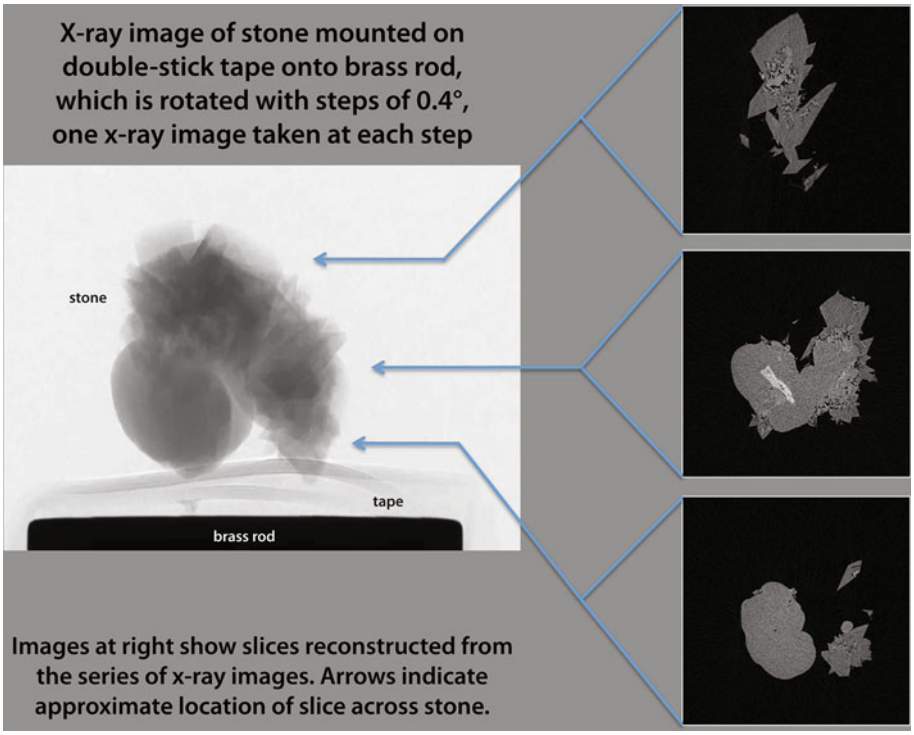

Fig. 2 Example of an X-ray 'shadow' image of a small kidney stone, along with reconstructed slices of the stone's interior, as calculated by the tomographic algorithm

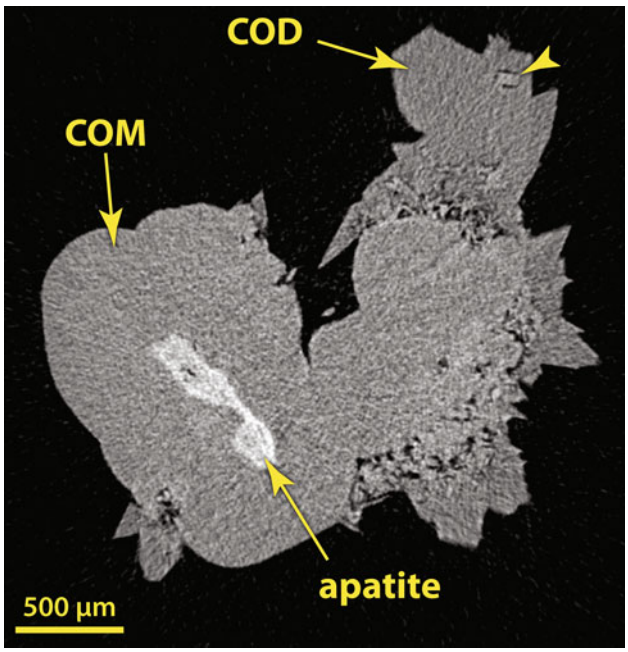

Fig. 3 Micro CT slice through the middle of the stone shown in Fig. 2. This stone was only 2 mm across, so the detail here is truly microscopic, with voxel sizes of 3.8 µm. Three mineral types can be seen by X-ray attenuation: calcium oxalate monohydrate (COM), calcium oxalate dihydrate (COD), and apatite (a form of calcium phosphate, probably more appropriately called 'carbapatite'). *Arrowhead* marks a region of apparent transformation of COD to COM

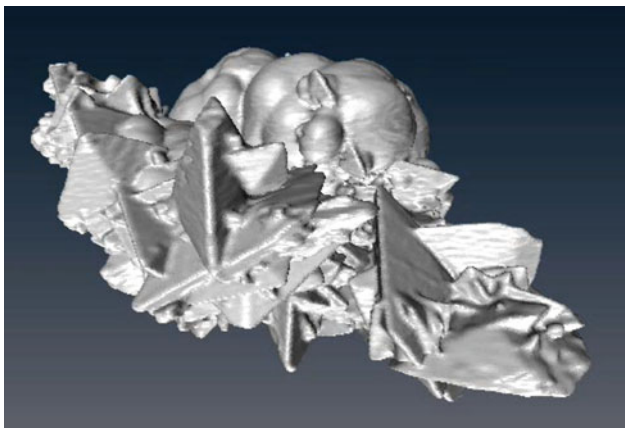

Fig. 4 Surface rendering of stone shown in Figs. 2, 3. The polyhedral shape of the COD crystals is apparent, as is the manner in which the crystals appear to be imbedded into one another ('twinning'). The smooth, rounded surface toward the back of the stone is the region dominated by COM (Fig. 3)

The main shell surrounding the stone in Fig. 5 (region 2) was found by FT-IR to be composed of apatite (with 12% carbonate); the low attenuating material (region 1) was not successfully recovered during dissection. The regions marked as 3 in Fig. 5 did not contain mineral on dissection, but were observed to be air spaces among the crystals of region 4; presumably these had been filled with urine (or perhaps protein as a thin gel) in vivo. Region 4 was composed of clear crystals, and these were shown by FT-IR to be pure COM. Regions 5 and 6 appeared to be a single layer on dissection, coal-black in color; this was found to contain COM plus apatite. The center of the stone (region 7) was amorphous and white in appearance on dissection,

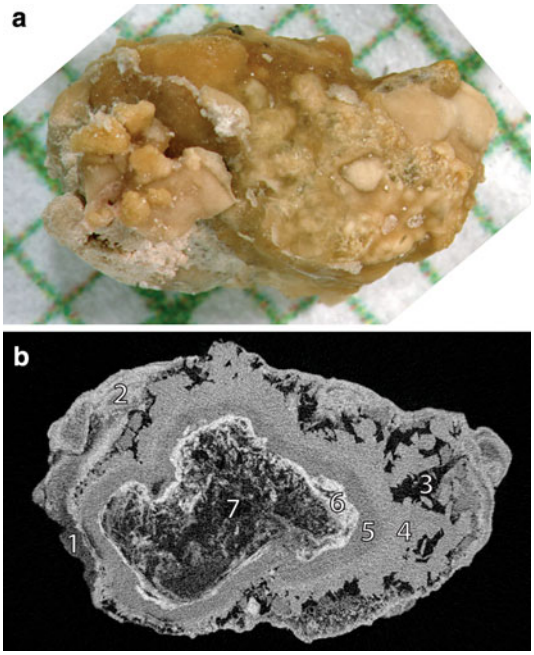

Fig. 5 Example of the complexity of mineral regions sometimes revealed by micro CT. **a** Photomicrograph of stone on millimeter grid paper. **b** Micro CT slice through the same stone. Mineral appears to be quite varied, as judged by morphology and X-ray attenuation; e.g., there is a low attenuation region on the stone exterior (labeled **1**) that is distinct from the high-attenuation shell surrounding the stone (**2**), beneath that shell are some regions that appear to be void of mineral (**3**), interspersed among crystalline extensions of an evenly absorbing material (**4**), inside this is a layer that absorbs X-rays less well (**5**), which is in turn lined by a highly absorbing mineral (**6**), finally, the innermost region of the stone (**7**) is filled with a low-absorbing material that could be subdivided into two or more morphologies. Details of subsequent dissection and analysis of stone is in text

and turned out to be composed of the calcium phosphate mineral, whitlockite, along with a fair amount of protein.

Thus, we can speculate about the history of the formation of the stone in Fig. 5: The stone began as a nidus of whitlockite, which has been associated with urinary tract infection [23, 24], and the relatively high concentration of protein seen in this region is also consistent with an infection origin. Following this, a layer of apatite (region 6) and then COM (regions 5 and then 4) was deposited. The first portion of the apatite and COM addition included an unknown pigment that stained the layers black and that made the COM less X-ray dense (region 5); perhaps this pigment was related to the treatment of urinary tract infection, but its identity has not been determined. The subsequent growth of COM (region 4) was initially slow—as evidenced by the tight, even appearance of the mineral—but then became more rapid, as shown by the large crystals seen at the surface of region 4. This period of calcium oxalate crystallization was then altered to one of apatite deposition, which could have been in response to dietary change; the carbonation level of the apatite (12%) was in the range that is less likely associated with infection [23].

Figure 5 provides just one example, but it demonstrates how micro CT imaging of a stone can improve the analysis of a stone by indicating regions that need to be dissected out and measured by another method. This example also shows how micro CT can illustrate the history of a stone's formation, a concept that has long been utilized to understand cross-sections of stones [25].

Screening stone fragments with micro CT

When a patient has a large stone burden, the material delivered for stone analysis is likely to include numerous fragments. While these fragments can be examined individually by stereomicroscopy and spectroscopic analysis, the process is tedious and quite time-consuming. Our practice has been to package groups of fragments together, wrapped in a paraffin film, and to scan them by micro CT as a group. It is then easy to scan through the image series and to quickly assess whether the fragments are uniform in CT appearance or not, and from there to make decisions on which fragments, and how many, should be followed up with dissection and spectroscopic work-up.

Figure 6 illustrates a case in which the fragments collected from the patient initially appeared to be uniformly composed of a common sort of apatite. However, micro CT revealed specific regions with a different morphology. As seen in Fig. 6b, most of the fragments consist of multiple light–dark layers that are typical of apatite [10]. Among these, though, were some regions that showed an evenness of texture and a medium X-ray attenuation value, the appearance commonly seen for COM. These identifications were then confirmed by spectroscopic analysis.

In such a case, one could easily envision a stone analysis report mentioning only the apatite content, as this material was predominant among the multiple fragments. Because this apatite was highly carbonated (42%), it would be easy for the physician to see this case as stone formation entirely related to an infectious event [23], and thus not to ask the patient to undergo a metabolic work-up for stones.

The finding of COM in this sample could change the picture from one of a patient with a single infection event to one of a calcium oxalate stone former who happened to have a concomitant urea-splitting infection. In the latter case, many physicians would recommend a metabolic work-up to identify a possible underlying metabolic abnormality that could be treated to reduce the risk of stone recurrence.

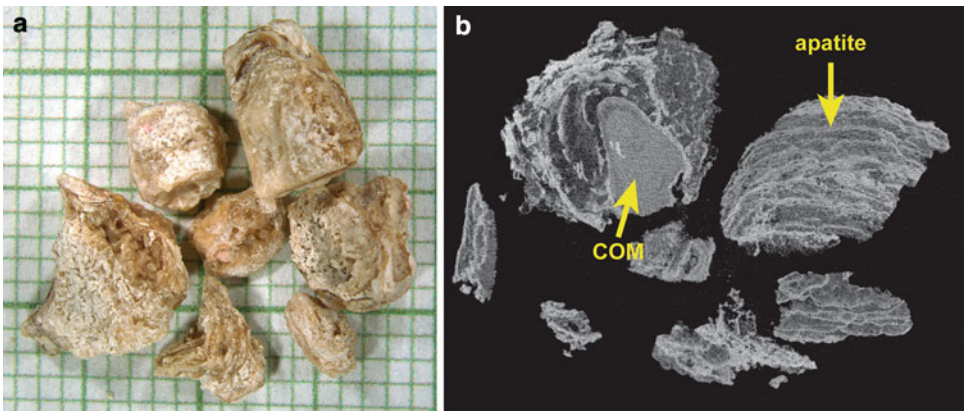

Fig. 6 Example of how a micro CT scan of stone fragments can reveal a minor stone component that might be missed during typical microscopic viewing and dissection. **a** Photomicrograph of stone fragments removed during percutaneous nephrolithotomy. Appearance of stone during surgical removal was consistent with stone being composed of apatite, and probably of infectious origin. Fragments show the white and brown layers characteristic of apatite laid down with calcium oxalate (Daudon's IIa+IVa [33]). **b** Micro CT slice through the same group of fragments. Although the layering of apatite (alternating layers of X-ray dense and less-dense material [10]) is seen in every fragment here, one fragment has a substantial piece of a material of even grayness, which is commonly seen in COM (Fig. 3). Subsequent analysis of this piece by FT-IR confirmed the presence of COM. The presence of such a piece of COM suggests that the patient is likely an oxalate stone former, even in the absence of infection

Using the 3D structure of stones for understanding etiology

One of the novel uses of micro CT for stones has been its application in understanding the way that different kinds of stones form. The first application of micro CT for understanding stone etiology was directed toward the idiopathic calcium oxalate stone former. The studies have shown that in idiopathic calcium oxalate patients most stones grow attached to papillae, on Randall's plaques [9]. The studies of idiopathic calcium oxalate patients also demonstrated that unattached stones all have interior inclusions of apatite, suggesting that their formation was likely also from Randall's plaque. Once the attached stone became dislodged the remnant of the plaque was covered by subsequent growth of calcium oxalate, creating the interior inclusion of apatite [26].

A brief presentation of the use of micro CT in the study of idiopathic calcium oxalate pathogenesis is shown in Fig. 7. Papillae with attached stones were imaged using a digital nephroscope before and after the stones were removed, and micro CT was used to describe the underside of the stone, with adhering apatite plaque, in relation to the papilla surface. The results provide powerful confirmation of Randall's theory in this type of stone patient. The stones were found to be firmly attached to Randall's plaque, which typically was pulled away from the papilla along with the stone. Micro CT allowed direct visual reconstruction of this connection, which otherwise is only inferred from the appearance of the stone [27, 28].

Figure 7a shows a papilla typical of the idiopathic calcium oxalate stone former, with a region of white plaque visible on the papilla surface above an attached stone. (Note that regions of Randall's plaque can remain covered by papillary epithelium, and thus persist without initiating stone growth [29], as the papillary epithelium prevents the plaque from coming into contact with urine.) The stone was removed, photographed, and then scanned by micro CT. The stone demonstrated a piece of apatite adherent to its underside, but where was that apatite when the stone was attached to the papilla?

Figure 7b shows a micro CT reconstruction of the stone that was matched to the position of the stone image in Fig. 7a. A picture of the papilla after the stone was removed was also oriented to match the parts of the papilla visible in Fig. 7a (plaque and a blood spot were both used as fiducial marks for this purpose). Note that the angle of the nephroscope was not identical between the before and after pictures, but the images of the papilla were matched as closely as possible, paying special attention to the regions close to the stone.

Figure 7b has the 3D micro CT reconstruction of the stone—shown in maximum-intensity projection mode so the apatite on the underside shows through as a white region—oriented to match the stone image in panel A, but placed above the oriented picture of the papilla post-stone removal.

Figure 7c shows the region of stone attachment with the apparent original position of the apatite that was adherent to the underside of the stone. The position is entirely consistent with the adherent apatite having originated as

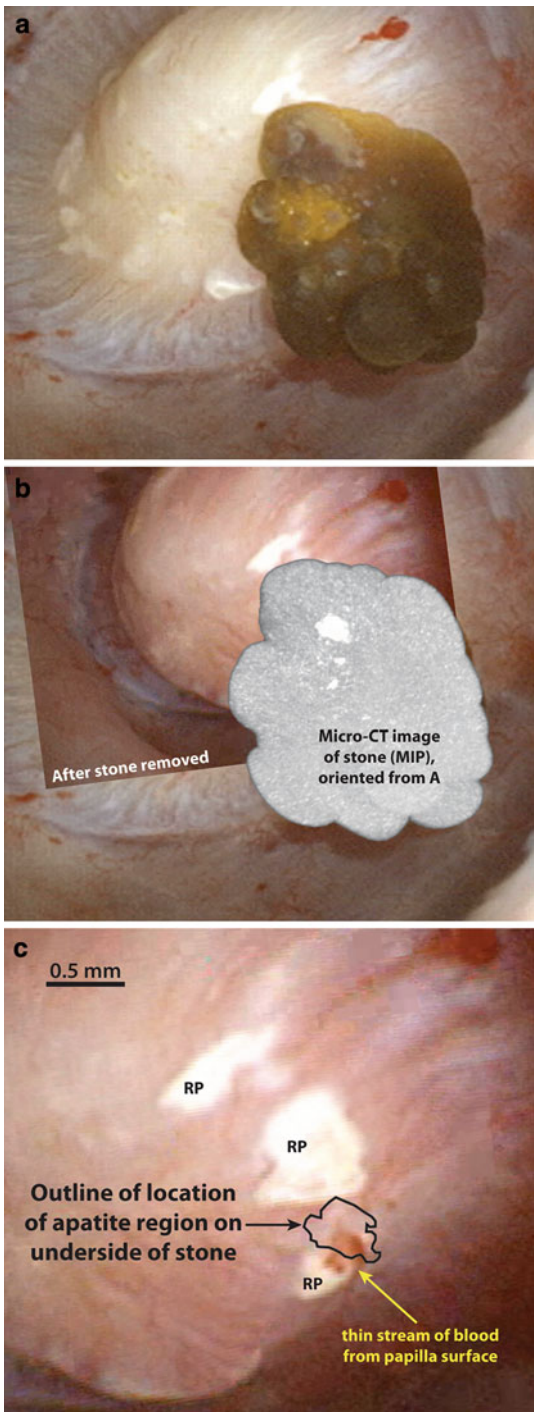

Fig. 7 Use of micro CT to identify attachment point of stone removed from idiopathic calcium oxalate stone former. **a** Nephroscope image of attached COM stone. **b** Image from **a** is overlaid with image of stone from micro CT (*gray overlay*) and image of papilla after stone was removed (*positioned underneath micro CT image*). **c** Blow-up of attachment site of stone on papilla. Outline shows patch of apatite found on underside of stone after removal. Position of this outline is consistent with apatite patch having been part of Randall's plaque (*RP*) in the tissue of the papilla, and that this portion of plaque was pulled away with the stone, causing some bleeding (*yellow arrow*)

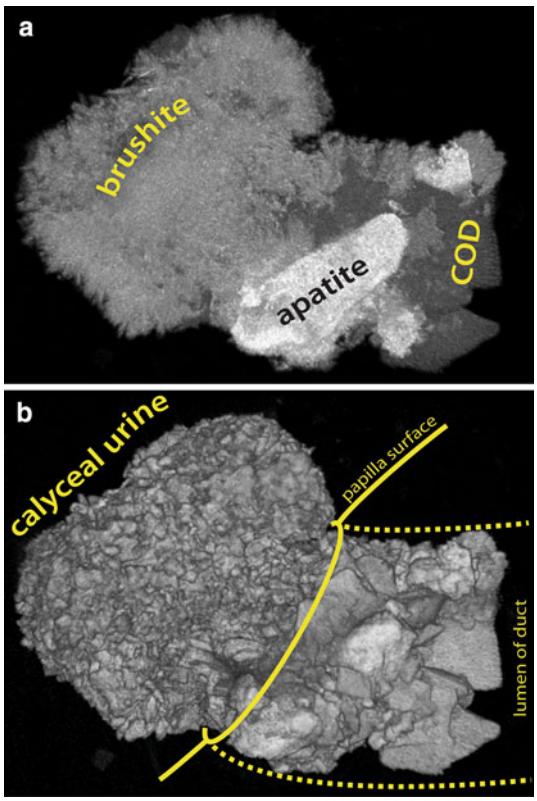

Fig. 8 Stone pulled from mouth of Bellini duct in brushite patient. Mineral identifications are made using X-ray attenuation [5] and crystal morphologies [10] from micro CT scan of stone (reconstructed using 4.15 μm voxels). **a** Maximum-intensity projection of 3D image stack. Bulk regions of brushite, apatite, and calcium oxalate dihydrate are marked. **b** Surface rendering of stone, with schematic of probable position of stone within tip of papilla. Note that mineral within duct is dominated by apatite and calcium oxalate, while mineral exposed to calyceal urine is mainly brushite

interstitial (Randall's) plaque that was in between other regions of plaque that remained on the papilla. There is even a trail of blood, apparently from the wound induced by pulling the stone away.

Figure 7 uses a different stone from that originally published with these data [9]. All of the stones examined in the above described manner demonstrated the same thing: The stones were connected to plaque on the papilla, and some of the plaque pulled away with the attached stone.

A different type of stone etiology is shown in Fig. 8. This stone was found protruding from the mouth of a duct of Bellini in a patient that formed brushite stones. This type of stone former is known to produce deposits of apatite within the lumens of the papillary collecting ducts [30]. It is possible that these deposits of apatite within the collecting ducts provide the initial, fixed sites for growth of brushite stones in this type of stone former, though evidence for this hypothesis is presently limited. Micro CT is just beginning to be used to study this type of patient.

Panel A of Fig. 8 shows a maximum-intensity projection of the stone, with mineral compositions inferred from previous experience. (The stone is only 1.7 mm long, and so spectroscopic analysis will have to be done using microscopic methods [31]). The identification of COD is almost certain, as the material has the correct X-ray attenuation value for this form of oxalate, along with its characteristic polygonal crystal shapes, which can be partly seen on the right side of the surface view in panel B. Apatite is characteristically the most X-ray absorbent material in stones, so the white regions in panel A are likely apatite. Finally, brushite often appears with radial distributions of crystals [10] and typically has an X-ray attenuation between that of calcium oxalate and apatite.

Thus, it appears that this stone consists of apatite and COD within the mouth of the collecting duct, and a ball of brushite growing on this into the calyceal space. This arrangement fits with the finding of apatite within the collecting ducts, but brushite within the urine, of brushite stone-forming patients [30]. The inferred position of the stone is shown in panel B.

The way in which brushite stones form is still not entirely clear, and the linkage between apatite deposition in the collecting ducts and the generation of brushite stones is only hypothetical [32], but micro CT will be an important tool to help understand this form of stone disease.

Stone analysis using micro CT

Micro CT is a powerful tool for stone analysis, providing a microscopic view of stones that is unavailable by any other method; one can see both the surface of the stone (as with SEM) and slices within the stone (as with ground sections of stones) but without any limits as to angle of view or section, and without damaging the stone in any way. All of the traditional methods for stone analysis can also be applied to the stone, but micro CT makes those methods more powerful by providing a structural map of the stone to guide further (destructive) forms analysis. Moreover, many minerals can be identified with confidence using micro CT alone.

Micro CT technology has not yet been utilized for commercial stone analysis, probably because of machine expense (about US $300,000) and because the time required for micro CT would add additional costs. However, if the cost of micro CT systems falls, commercial laboratories might find it a valuable addition that could save time in analysis of some specimens—especially in screening large groups of fragments. Micro CT also adds accuracy for at least some analyses; specifically, total volumes of apatite (as a minor component) can be easily determined for some stone types using micro CT, a measure that is quite difficult to do accurately by traditional methods [15].

For research in stone disease, micro CT provides benefit in a wide variety of study types. Studies of stone etiology were highlighted above, but any clinical study in which stone analysis is done could reduce errors in identification of stone type by adding micro CT to their protocols [15]. For any longitudinal study of stone patients, micro CT offers the possibility of matching the history of a patient to the history of mineral deposition in the stones (as described for Fig. 5 above), which could be an excellent way to confirm or refute hypotheses about the effects of medical management on stone growth. For in vitro studies of stones, micro CT is now essential for ensuring that stones studied are indeed of the composition expected. Ensuring proper stone composition is imperative for studies focusing on the clinical CT assessment of stone composition [11], and for studies of stone fragility in shock wave lithotripsy [14]. In such studies, the stones used are typically cohort stones left over after a stone analysis, and as such can differ significantly from the stone pieces that were actually analyzed (not to mention the possibility that the analysis may be incorrect [15]).

In sum, micro CT provides an analysis tool for urinary stones that has great power, adds value to existing methods and also adds new capabilities that were previously unavailable. Its value for routine, clinical stone analysis is still untapped, but as a research tool its role is already evident and will likely increase.

Acknowledgments Funded in part by NIH R01DK059933, S10 RR023710, and P01 DK565788.

References

1. Muller R, Hahn M, Vogel M et al (1996) Morphometric analysis of non-invasively assessed bone biopsies: comparison of high-resolution computed tomography and histologic sections. [Erratum appears in Bone 1996 Sep; 19(3):299]. Bone 18:215–220
2. Ruegsegger P, Koller B, Muller R (1996) A microtomographic system for the nondestructive evaluation of bone architecture. Calcif Tissue Int 58:24
3. Ritman EL, Bolander ME, Fitzpatrick LA et al (1998) Micro-CT imaging of structure-to-function relationship of bone micro-structure and associated vascular involvement. Technol Health Care 6:403
4. Cleveland RO, McAteer JA, Müller R (2001) Time-lapse non-destructive assessment of shock wave damage to kidney stones in vitro using micro-computed tomography. J Acoust Soc Am 110:1733
5. Zarse CA, McAteer JA, Sommer AJ et al (2004) Nondestructive analysis of urinary calculi using micro computed tomography. BMC Urol 4:15
6. Zarse CA, McAteer JA, Tann M et al (2004) Helical CT accurately reports urinary stone composition using attenuation values: In vitro verification using high resolution micro CT calibrated to FT-IR microspectroscopy. Urology 63:828

7. Kim SC, Hatt EK, Lingeman JE et al (2005) Cystine: helical computerized tomography characterization of rough and smooth calculi in vitro. J Urol 174:1468
8. Matlaga BR, Williams JC Jr, Evan AP et al (2007) Calcium oxalate stones are frequently found attached to Randall's plaque. In: Evan AP, Lingeman JE, Williams JC Jr (eds) Renal stone disease. Proceedings of the First International Urolithiasis Research Symposium. American Institute of Physics, Melville, NY, pp 35–41
9. Miller NL, Gillen DL, Williams JC Jr et al (2009) A formal test of the hypothesis that idiopathic calcium oxalate stones grow on Randall's plaque. BJU Int 103:966
10. Pramanik R, Asplin JR, Jackson ME et al (2008) Protein content of human apatite and brushite kidney stones: significant correlation with morphologic measures. Urol Res 36:251
11. Primak AN, Fletcher JG, Vrtiska TJ et al (2007) Non-invasive differentiation of uric acid versus non-uric acid kidney stones using dual-energy CT. Acad Radiol 14:1441
12. Williams JC Jr, Matlaga BR, Kim SC et al (2006) Calcium oxalate calculi found attached to the renal papilla: Preliminary evidence for early mechanisms in stone formation. J Endourol 20:885
13. Williams JC Jr, Zarse CA, Jackson ME et al (2006) Variability of protein content in calcium oxalate monohydrate stones. J Endourol 20:560
14. Zarse CA, Hameed TA, Jackson ME et al (2007) CT visible internal stone structure—but not Hounsfield unit value—of calcium oxalate monohydrate (COM) calculi predicts lithotripsy fragility in vitro. Urol Res 35:201
15. Krambeck AE, Khan NF, Jackson ME et al (2010) Inaccurate reporting of mineral composition by commercial stone analysis laboratories: implications for infection and metabolic stones. J Urol 184:1543
16. Ritman EL (2004) Micro-computed tomography-current status and developments. Annu Rev Biomed Eng 6:185
17. Feldkamp LA, Davis LC, Kress JW (1984) Practical cone-beam algorithm. J Opt Soc Am A 1:612
18. Hesse A, Berg W, Bothor C (1979) Scanning electron microscopic investigations on the morphology and phase conversions of uroliths. Int Urol Nephrol 11:11
19. Kim KM, Johnson FB (1981) Calcium oxalate crystal growth in human urinary stones. Scan Electron Microsc III:147–154
20. Cifuentes Delatte L, Hidalgo A, Bellanato J et al (1973) Polarization microscopy and infrared spectroscopy of thin sections of calculi. In: Cifuentes Delatte L, Rapado A, Hodgkinson A (eds) Urinary Calculi. Recent advances in aetiology, stone structure and treatment, S. Karger, Basel pp 220–230
21. Schubert G, Brien G (1981) Crystallographic investigations of urinary calcium oxalate calculi. Int Urol Nephrol 13:249
22. Domingo-Neumann RA, Ruby AL, Ling GV et al (2001) Ultrastructure of selected calcium oxalate-containing urinary calculi from dogs. Am J Vet Res 62:237
23. Carpentier X, Daudon M, Traxer O et al (2009) Relationships between carbonation rate of carbapatite and morphologic characteristics of calcium phosphate stones and etiology. Urology 73:968
24. Maurice-Estepa L, Levillain P, Lacour B et al (1999) Crystalline phase differentiation in urinary calcium phosphate and magnesium phosphate calculi. Scand J Urol Nephrol 33:299
25. Carter HV (1873) The microscopic structure and mode of formation of urinary calculi J. & A. Churchill, London
26. Miller NL, Williams JC, Evan AP et al (2010) In idiopathic calcium oxalate stone-formers, unattached stones show evidence of having originated as attached stones on Randall's plaque. BJU Int 105:242
27. Cifuentes Delatte L, Miñón Cifuentes J, Medina JA (1996) Randall and his plaque. Urology 48:343
28. Cifuentes Delatte L, Miñón-Cifuentes JL, Medina JA (1985) Papillary stones: calcified renal tubules in Randall's plaques. J Urol 133:490
29. Evan AP, Lingeman JE, Coe FL et al (2003) Randall's plaque of patients with nephrolithiasis begins in basement membranes of thin loops of Henle. J Clin Invest 111:607
30. Evan AP, Lingeman JE, Coe FL et al (2005) Crystal-associated nephropathy in patients with brushite nephrolithiasis. Kidney Int 67:576
31. Anderson JC, Williams JC Jr, Evan AP et al (2007) Analysis of urinary calculi using an infrared microspectroscopic surface reflectance imaging technique. Urol Res 35:41
32. Krambeck AE, Handa SE, Evan AP et al (2010) Brushite stone disease as a consequence of lithotripsy? Urol Res 38:293
33. Daudon M, Bader CA, Jungers P (1993) Urinary calculi: review of classification methods and correlations with etiology. Scanning Microsc 7:1081